NATIONAL ADVISORY COMMITTEE FOR AERONAUTICS

TECHNICAL NOTE 3903

AN EXPERIMENTAL HYDRODYNAMIC INVESTIGATION

OF THE INCEPTION OF VORTEX VENTILATION

By John A. Ramsen

Langley Aeronautical Laboratory
Langley Field, Va.

NACA

Washington
April 1957

1L

NATIONAL ADVISORY COMMITTEE FOR AERONAUTI

TECHNICAL NOTE 3903

AN EXPERIMENTAL HYDRODYNAMIC INVESTIGATION

OF THE INCEPTION OF VORTEX VENTILATION

By John A. Ramsen

SUMMARY

An experimental hydrodynamic investigation of some of the parameters affecting the inception of vortex ventilation has been conducted on three modified flat plates of aspect ratio 0.25 differing in scale and thickness ratio.

For all three models, two distinct bubble-formation processes were noted. The speed of inception of the planing bubble in the high angle-of-attack range varied only slightly with angle of attack but increased considerably with increasing depth of submersion. Correlation of this inception speed for all three models was accomplished by using the Froude number and the depth in chords at the leading edge measured to the center line of the longitudinal cross section.

The speed of inception of the planing bubble in the low angle-of-attack range increased significantly with decreasing angle of attack and only slightly with increasing depth of submersion. The speed of inception for the two models differing only in scale was the same, whereas the model differing in thickness ratio was brought into correlation by expressing the speed as a function of the thickness ratio.

INTRODUCTION

A series of investigations have been conducted by the National Advisory Committee for Aeronautics to determine the force and moment characteristics of submerged low-aspect-ratio lifting surfaces. In the course of these investigations (reported in refs. 1 to 3) flow separation at the leading edge following ventilation through the trailing vortices occurred at the higher angles of attack for shallow depths of submersion. This separation was found, in the tests of reference 1, to assume one of two forms: white water, which caused only slight changes in the force and moment characteristics; and the planing bubble, which caused a sharp drop in both the forces and the moments.

Since a drop such as that caused by the planing bubble would be of considerable importance in any practical application of the lifting surfaces, an investigation to determine some of the parameters affecting the inception of this vortex ventilation was initiated. This paper presents the results of an experimental investigation conducted in Langley tank no. 2 on three modified flat plates of aspect ratio 0.25. The first model was one that had been used in the tests of reference 1, the second model was a 2.546-scale model of the first model, and the third model was one with the same plan form but twice the thickness of the first model.

Two distinct bubble-formation processes observed during the tests are discussed, and a method is presented which accounts for the effects of scale and thickness on the inception of ventilation.

<div align="center">SYMBOLS</div>

b span of lifting surface, ft

C_L lift coefficient, $\dfrac{L}{\frac{\rho}{2}V^2bc}$

c model chord, ft

c_s strut chord, ft

d depth of submersion measured from free water surface to point on model closest to the surface, ft

d' depth of submersion measured from free water surface to center line of longitudinal cross section at leading edge, ft

N_{Fr} Froude number, $\dfrac{V}{\sqrt{gc}}$

g acceleration due to gravity, 32.2 ft/sec^2

L lift force, lb

t model thickness, ft

V forward velocity, fps

α angle of attack, deg

ρ mass density of water, 1.942 slugs/cu ft for these tests

APPARATUS AND PROCEDURE

Description of Models

Details of the models tested are shown in figure 1. In all three cases the models were of aspect ratio 0.25 and were mounted on a single strut having an NACA 66_1-012 airfoil section. The model leading edges were rounded to a 2:1 ellipse, and the trailing edges were symmetrically beveled to provide an included angle of 10°.

For purposes of identification, the three models have been designated herein the small model, the large model, and the thick model. The small model was used in the tests of reference 1 and was made as thin as possible in order to get as close an approximation to a true flat plate as possible. Because the model was to be used with a balance that had a small load capacity it was designed to carry only those loads up to the balance capacity. The large model was constructed as an exact scale model of the small model, the scale being the ratio of 36.00 to 14.14 or approximately 2.546. This model was constructed specifically for the present investigation to determine the effects of scale on ventilation. The thick model was constructed for the tests of reference 3, which were made to extend the range of speeds over which the small model had been tested. In order to keep the deformation of the model small under the increased loads accompanying this increase in speed range, this model had to be made twice as thick as the small model. In order to maintain the plan-form shape, the elliptical leading edge, and the beveled trailing edge of the other models, the leading-edge radius of the thick model was necessarily increased, and the leading- and trailing-edge modifications proportionately increased.

The dimensions of the struts used to support the three models were dictated by the amount of strength necessary to take the expected loads. Therefore, although all the struts were of the same airfoil section, they varied in chord and in thickness. This variation in strut size, of course, affected the drag, but the tests of reference 2 indicated that the total effect of the strut on the lift was small. Thus, any variation in the strut dimensions could be considered a second-order effect as far as the lift was concerned and could be neglected. The tests of reference 2 also indicated that the strut had a negligible effect on the formation of the planing bubble. This lack of effect was confirmed in some short check tests made in the course of this investigation.

Test Methods and Equipment

Tests were made in Langley tank no. 2, for which the towing carriage was equipped with a wind screen to reduce aerodynamic tares and aerodynamic effects on flow patterns to negligible values. Measurements of lift were made by use of an electrical strain-gage balance.

Lift measurements were taken at constant speeds for fixed angles of attack and depths of submersion. The depth of submersion is defined as the distance from the free water surface to the point on the model nearest that surface. Depths of submersion of 0.5 inch and 1.0 inch were used for each angle of attack investigated, and the depth was then increased in 1.0-inch increments until no ventilation was encountered in the available speed range. Similarly, the angles of attack covered at a given depth ranged from 20° down to the angle for which no ventilation occurred at that depth. The range of speeds covered for the large model and for the thick model extended up to 85 feet per second. Speeds for the small model were limited to those for which bending and vibration were no problem.

Changes in depth of submersion and angle of attack were small because of the structural rigidity of the supporting system. Estimated accuracies for the data presented are:

Angle of attack, deg . . . . ±0.1
Depth of submersion, in. . . . . ±0.05
Lift, lb . . . . ±2.5
Speed, ft/sec . . . . ±0.2

The lift force was converted to coefficient form by using a measured value of the density of water of 1.942 slugs/cu ft. The kinematic viscosity measured during the tests was 1.20×10^{-5} sq ft/sec.

RESULTS AND DISCUSSION

Description of Ventilation and Its Effects

In the tests of reference 1, at the higher angles of attack and the shallower depths of submersion, air was observed to enter the trailing vortices aft of the model. As the speed was increased, the entrained air proceeded forward along a helical path inside the vortices until it reached the model, when flow separation took place. This process, in which the flow takes the form of a fully ventilated planing bubble (an air bubble surrounded by a film of water in such a manner that the water does not touch the upper surface of the model) is shown schematically in figure 2. This form of separation was found in reference 1 to occur for

the lifting surfaces having aspect ratios of 0.25 and 0.125. For the model of reference 1 having an aspect ratio of 1.00 the separation generally took the form of white water, a foamy mixture of air and water covering the upper surface of the model. With increasing speed this white water changed into the planing bubble.

Bubble Formation

Because all three models used in the tests described in this paper had aspect ratios of 0.25, the planing-bubble type of separation would be expected to occur. However, two distinct types of bubble formation were noted, even though both finally resulted in the planing bubble. One was associated with high angles of attack and the other with low angles of attack.

High-angle bubble.- The formation which occurred for higher angles of attack than did the other is called the high-angle bubble and is illustrated in the photographs of figure 3 for the large model. At a speed of 5 feet per second the flow is smooth, and no evidence of air in the vortices can be noted. At a speed of 10 feet per second air has entered the vortices and proceeded forward on both sides of the model to a point forward of the strut. Separation at the leading edge has already occurred at a speed of 12.5 feet per second, and a partially ventilated bubble called a partial bubble is formed, beginning at the leading edge. Reflection of the lights from the surface of this bubble may be seen in the photograph. At this speed the flow has reattached at a point near the trailing edge of the strut and formed a partial bubble. At a speed of 15 feet per second the reattachment point has moved farther aft to a position near the trailing edge of the model, and the bubble has expanded somewhat. The partial bubble has changed to the fully ventilated planing bubble (called a full bubble) at a speed of 17.5 feet per second, and the bubble has expanded considerably. At a speed of 22.5 feet per second the bubble has further expanded and extends out of the photographed area aft of the model. This series of photographs was obtained with the large model, but the flow processes accompanying the formation of this high-angle type of bubble were identical for all three models.

In the process of changing from the partial bubble to the full bubble, a fairly large amount of aerated water flowed forward under the bubble on the upper surface of the model. This action occurred at a speed of approximately 17.5 feet per second, although it cannot be clearly seen in the photograph. From visual observation, however, the flow was seen to be very similar to that of the white water found for the model with an aspect ratio of 1.00 in the tests of reference 1. This similarity leads to the supposition that the white water was simply another form of the partial bubble since it too changed to the full bubble with an increase in speed.

The lift force in pounds is shown in figure 4 as a function of the speed for the large model at an angle of attack of 16° and a depth of submersion of 0.5 inch (the case illustrated in fig. 3). Also included in this figure are lift-force data for submersion depths of 1.0 inch and 2.0 inches. The single arrows indicate the lowest speeds at which data were taken with the partial bubble present, and the double arrows indicate the first appearance of the full bubble. Initial occurrence of the bubbles is thus located between the arrowed speed and the test speed next below it. The curves drawn in this figure are the result of a cross fairing against angle of attack. For the 0.5-inch depth, illustrated in figure 3, the partial bubble was present at a speed of 11 feet per second and the full bubble at a speed of 16.5 feet per second. The speeds at which the bubbles occurred increased with increasing depth as might be expected. It is interesting to note that before formation of the full bubble the lift decreased with decreasing depth of submersion as a result of the free-surface effects, whereas after formation of the full bubble the lift values appeared to fall on a single line regardless of depth and indicated the absence of surface effects.

Formation of the partial bubble had little or no effect on the lift force for any depth. For the 0.5-inch and 1.0-inch depths the lift force continued to increase at about the same rate after formation of the partial bubble until the reattachment point had almost reached the trailing edge. Little change in lift force then occurred until the full bubble appeared, after which the lift again increased at a steady rate. At a depth of submersion of 2.0 inches no region of constant lift force was evident, and the lift dropped abruptly to the full-bubble value. Neither the small change in lift force preceding the full bubble at the shallow depths nor the partial bubble itself were recognized in the tests reported in reference 1, probably because the speeds at which data were taken were too widely separated. It might also be noted that the occurrence of the white water in the tests of reference 1 resulted in about the same lift behavior as the partial bubble noted here and gave a further indication that white water is probably a form of partial bubble.

Low-angle bubble.- The formation which occurred at the lower angles of attack is called the low-angle bubble and is shown in figure 5. In this formation the partial bubble does not occur, and the full bubble occurs at the first separation for this case. At a speed of 10 feet per second the flow is smooth, whereas at a speed of 20 feet per second the entrained air has proceeded forward within the vortices to a point just aft of the strut. At speeds of 35 feet per second and 40 feet per second the entrained air has moved farther forward, and the vortices have expanded in size. Also, at a speed of 40 feet per second the widening of the bright area at the leading edge indicates the presence of cavitation. At a speed of 50 feet per second ventilation and cavitation have both become stronger. The full bubble occurs before the speed of 70 feet per second is reached and eliminates both the aerated vortices and the cavitation.

Force data for the large model at an angle of attack of 8° and depths of submersion of 0.5 inch, 1.0 inch, and 2.0 inches are shown in figure 6. As in figure 4, the curves are the results of a cross fairing, and the double arrows indicate the data point at the lowest speed for which the full bubble was present. Since no partial bubble occurred, the lift force increased smoothly with increasing speed until the full bubble was formed, and a sharp drop in the lift occurred. Once again the lift decreased with decreasing depth of submersion until the separation occurred, which indicated the effect of the free surface. After separation, the values of the lift for all depths fell on the same line and indicated the absence of surface effects.

Similarity to Aerodynamic Stalling

The two types of bubble formation noted seem to have some similarity to two of the classifications of stalling cited in reference 4. The high-angle-bubble flow pattern resembles the thin-airfoil stall, which is described as being "preceded by flow separation at the leading edge with reattachment at a point which moves progressively rearward with increasing angle of attack". The present tests were made by increasing speed rather than angle of attack. The reattachment point in this case moved aft with increasing speed. The low-angle-bubble flow pattern resembles the leading-edge stall described as "abrupt flow separation near the leading edge generally without subsequent reattachment". Because of this similarity to the stall phenomena, some of the discussion of the boundary-layer phenomena governing the two types of separation presented in reference 4 may be applicable to this case. Of course cavitation and free-surface effects are also involved in this case.

Lift-Coefficient Data

The lift-coefficient data for the three models at the depths investigated are shown in figures 7, 8, and 9. The lift coefficients are plotted against speed with angle of attack and depth of submersion as parameters. As in the previous force plots, a single arrow indicates the lowest speed for the partial bubble, and a double arrow indicates the lowest speed for the full bubble. For both the small and the thick models (figs. 7 and 9) no separation was found at a depth of submersion of 2.0 inches; therefore, for these models data are presented for only 0.5-inch and 1.0-inch depths. For the large model (fig. 8) separation was not found at the 6.0-inch depth; therefore, data for this model are presented for depths up to 5.0 inches.

The lift coefficients generally show little change with the formation of the partial bubble. The gradual change to the full-bubble lift value noted in the force plots (fig. 4) is shown as a change in the

direction of the curve at some speed after the formation of the partial
bubble. This speed moves to higher values, in relation to the first
partial-bubble speed, as the depth of submersion is increased. At an
angle of attack of 14° for several of the conditions, the surging for-
ward under the bubble of the white water, mentioned in the previous sec-
tion, occurred at the time of transition from the partial bubble to the
full bubble and apparently was the cause of oscillation of the lift coef-
ficient between two values over a short range of speed. This phenomenon
is indicated by a shaded area in the plots. _(See, for example, figs. 7(b)
and 8(b).) As in the force plots, the low-angle type of bubble formation
gives a smooth curve up to the speed at which the full bubble appears
when a sharp break in the value of the lift coefficient occurs. It can
be seen from these plots that the speeds at which the full bubble occurs
vary only slightly with angle of attack for the high-angle type of bubble
formation but shift to much higher values and vary significantly with
angle of attack for the low-angle type.

Correlation of Ventilation Speeds

The ventilation boundaries, as defined by the appearance of the full
bubble, are shown in figure 10 by plots of angle of attack against speed,
with depth of submersion as a parameter. The definite separation between
the high-angle and the low-angle types of bubble formation can be seen
for each of the three models. The relatively small change with angle of
attack of the speed at which the full bubble occurs, in the case of the
high-angle bubble, is evident in this figure. The change of inception
speed with depth of submersion is appreciable, however, and increases
rapidly with increasing depth of submersion. Over a short range of angle
of attack near the separation between the high-angle and the low-angle
types of bubbles, the boundaries are somewhat erratic and vary over a
range of speeds for a given angle of attack. For the two models varying
only in scale and therefore of the same thickness ratio, the angle of
attack marking the separation remained the same (figs. 10(a) and (b)).
The increase in thickness ratio for the thick model raised this angle of
attack appreciably.

For the low-angle bubble a significant change with angle of attack
occurred in the ventilation speed. The change with depth of submersion
was, on the other hand, reduced to a small value. Attempts to determine
a method of correlating the ventilation speeds for the three models to
include both the high-angle and low-angle bubbles were unsuccessful.
Therefore, the two types of bubbles were investigated individually.

For regions where gravity is of importance the Froude method of
correlating is a standard procedure. It was found that the inception
of the high-angle bubble could be correlated for the large and the small
(geometrically similar) models by using the Froude number. The thick

model could be brought into correlation by choice of the proper depth of submersion reference. This choice was made by using the depth of submersion in chords measured to the longitudinal center line of the model at the leading edge rather than to the top of the model. Since little change occurred in ventilation speed with angle of attack for the high-angle type of bubble, a single average speed was analyzed for each depth for the range of angles involved. A plot of the Froude number against the depth parameter (fig. 11) shows that the data for all three models lie along one line. Apparently the thickness is of minor importance only, and the location (relative to the free water surface) of the vortex system for the model is the more important factor in this case.

Comparison of the speeds of inception of the low-angle bubble indicated that the small and the large models, which differed in scale but not in thickness ratio, had the same inception speeds (figs. 10(a) and (b)). The thick model, on the other hand, had a different inception speed; this difference indicated, therefore, that some parameter dependent on the thickness ratio was important for this case. The three models could be correlated by expressing the velocity as a function of the thickness ratio $\dfrac{V}{\sqrt{t/c}}$ and by using the depth of submersion measured to the top of the model. This agreement is shown in figure 12 for depths of submersion of 0.5 inch and 1.0 inch since data for all three models are available at only these depths.

CONCLUSIONS

An experimental hydrodynamic investigation of some of the parameters affecting the inception of vortex ventilation conducted on three modified flat plates of aspect ratio 0.25 differing in scale and thickness ratio indicated that:

1. Two distinct bubble-formation processes existed which showed some similarity to two of the types of stalling noted in aerodynamic investigations. The process which occurred for the higher angles of attack and is called the high-angle bubble was preceded by flow separation at the leading edge, and reattachment was at a point which moved aft with increasing speed. Little change in lift was found for separation with reattachment on the model, but the change to the full bubble, which occurred as the reattachment point reached the trailing edge, caused a rather large lift decrease. The process which occurred for the lower angles of attack and is called the low-angle bubble occurred as an abrupt flow separation at the leading edge without subsequent reattachment. The resulting full bubble again caused much lower lift than for the unseparated flow.

2. The speed of inception of the high-angle bubble varied only slightly with angle of attack but increased considerably with increasing

depth of submersion. Correlation of the inception speeds for the three models was obtained by using the Froude number $\dfrac{V}{\sqrt{gc}}$ and the depth in chords measured to the center line of the longitudinal cross section.

3. The speed of inception of the low-angle bubble increased significantly with decreasing angle of attack and slightly with increasing depth of submersion. The models differing only in scale gave the same inception speeds at the same absolute depths of submersion. Correlation for the models differing in thickness ratio was obtained by expressing the velocity as a function of the thickness ratio $\dfrac{V}{\sqrt{t/c}}$.

Langley Aeronautical Laboratory,
    National Advisory Committee for Aeronautics,
        Langley Field, Va., October 2, 1956.

<div style="text-align:center">REFERENCES</div>

1. Wadlin, Kenneth L., Ramsen, John A., and Vaughan, Victor L., Jr.: The Hydrodynamic Characteristics of Modified Rectangular Flat Plates Having Aspect Ratios of 1.00, 0.25, and 0.125 and Operating Near a Free Water Surface. NACA Rep. 1246, 1955. (Supersedes NACA TN's 3079 by Wadlin, Ramsen, Vaughan and 3249 by Ramsen and Vaughan.)

2. Ramsen, John A., and Vaughan, Victor L., Jr.: Hydrodynamic Tares and Interference Effects for a 12-Percent-Thick Surface-Piercing Strut and an Aspect-Ratio-0.25 Lifting Surface. NACA TN 3420, 1955.

3. Vaughan, Victor L., Jr., and Ramsen, John A.: Hydrodynamic Characteristics Over a Range of Speeds up to 80 Feet Per Second of a Rectangular Modified Flat Plate Having an Aspect Ratio of 0.25 and Operating at Several Depths of Submersion. NACA TN 3908, 1957.

4. McCullough, George B., and Gault, Donald E.: Examples of Three Representative Types of Airfoil-Section Stall at Low Speed. NACA TN 2502, 1951.
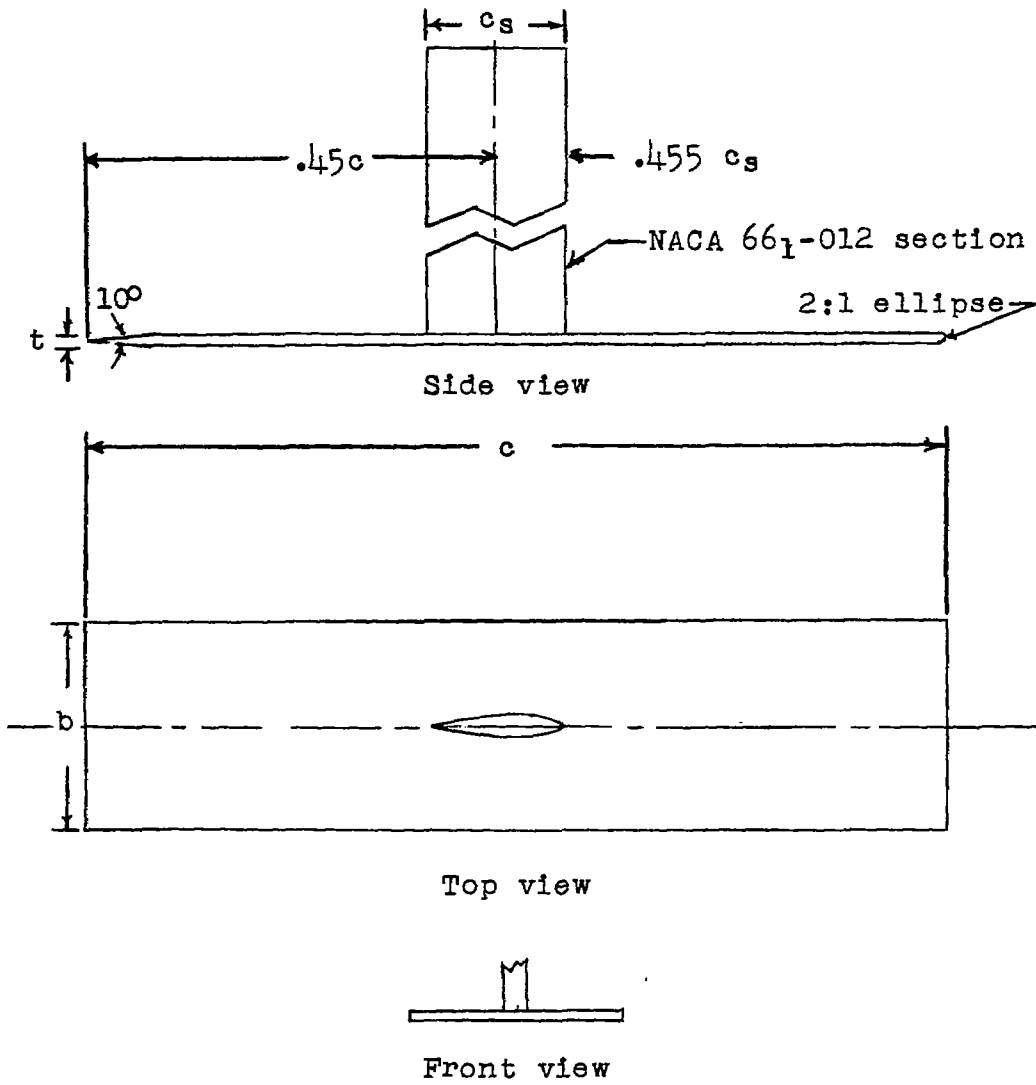
Figure 1.- Details of models. (Dimensions are in inches.)
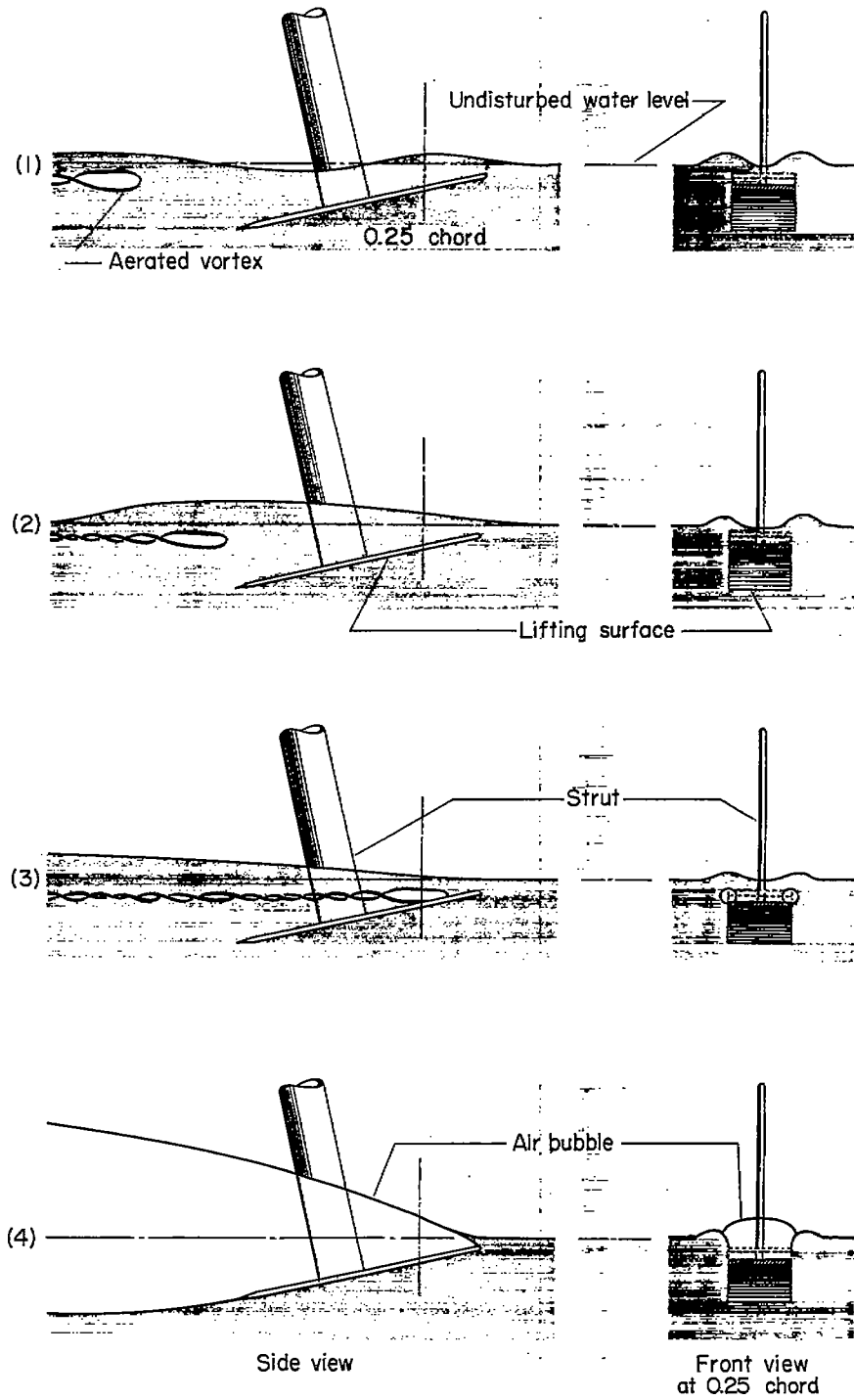
Figure 2.- Development of vortex ventilation.

5 fps
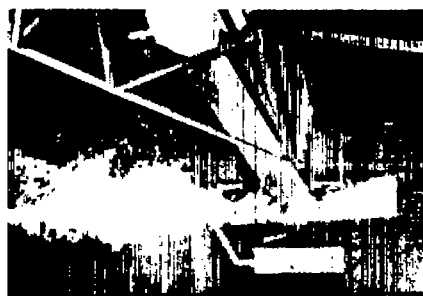
10 fps
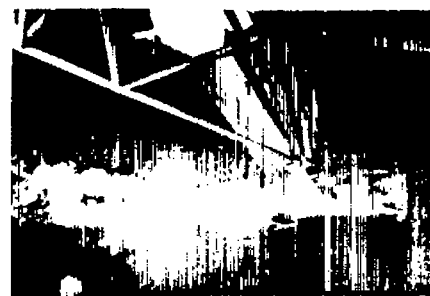
12.5 fps

15 fps
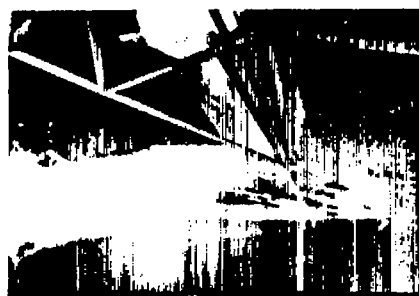
17.5 fps
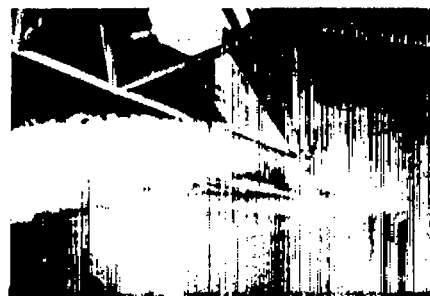
22.5 fps

L-95871

Figure 3.- Sequence photographs showing formation of high-angle bubble
for large model. (Angle of attack, 16°; depth of submersion,
0.5 inch.)
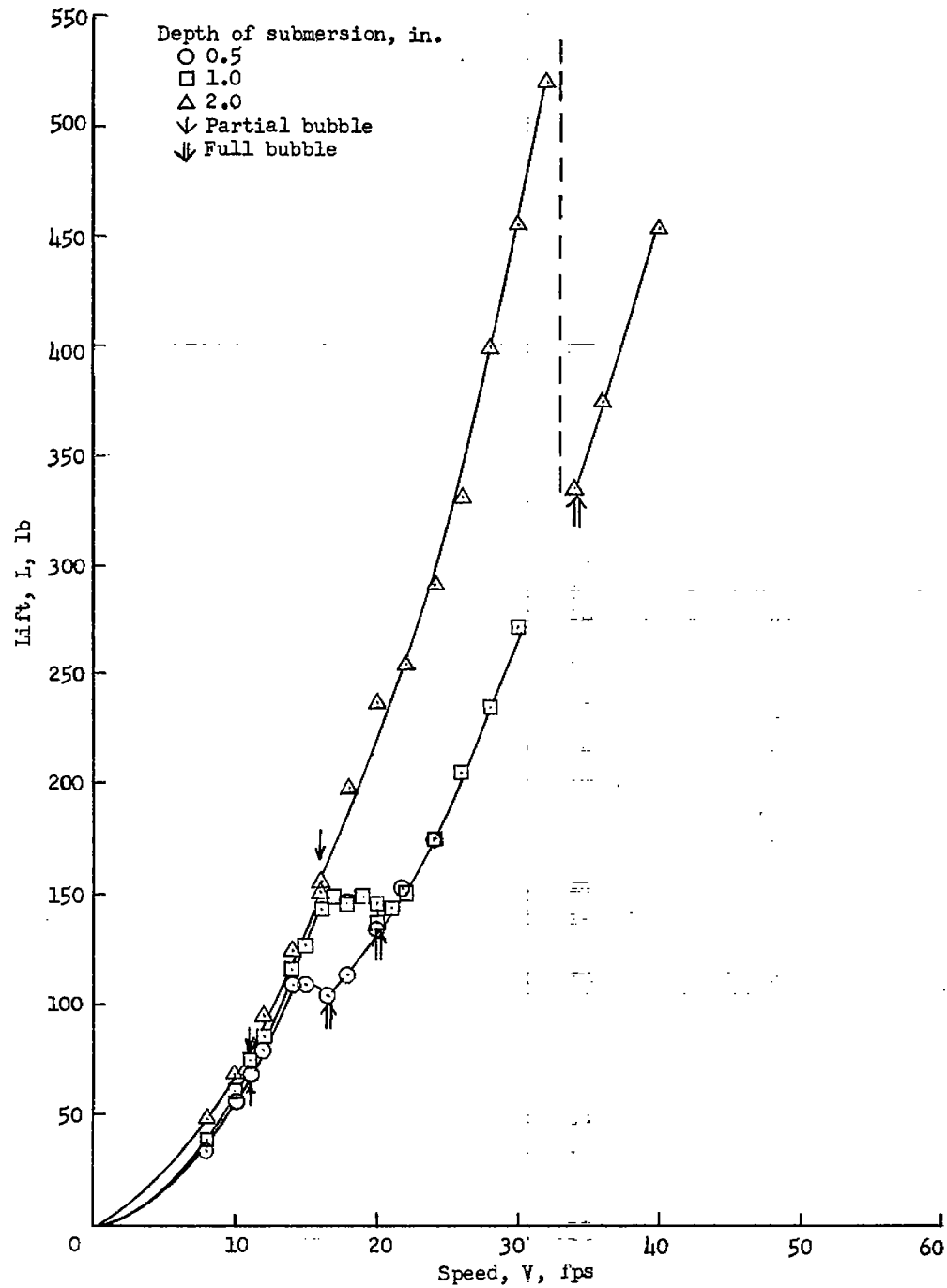
Figure 4.- Lift-force data for large model illustrating effects of high-angle bubble. (Angle of attack, 16°.)

10 fps

20 fps

35 fps

40 fps

50 fps

70 fps

L-95872

Figure 5.- Sequence photographs showing formation of low-angle bubble
for large model. (Angle of attack, $8°$; depth of submersion, 0.5 inch.)
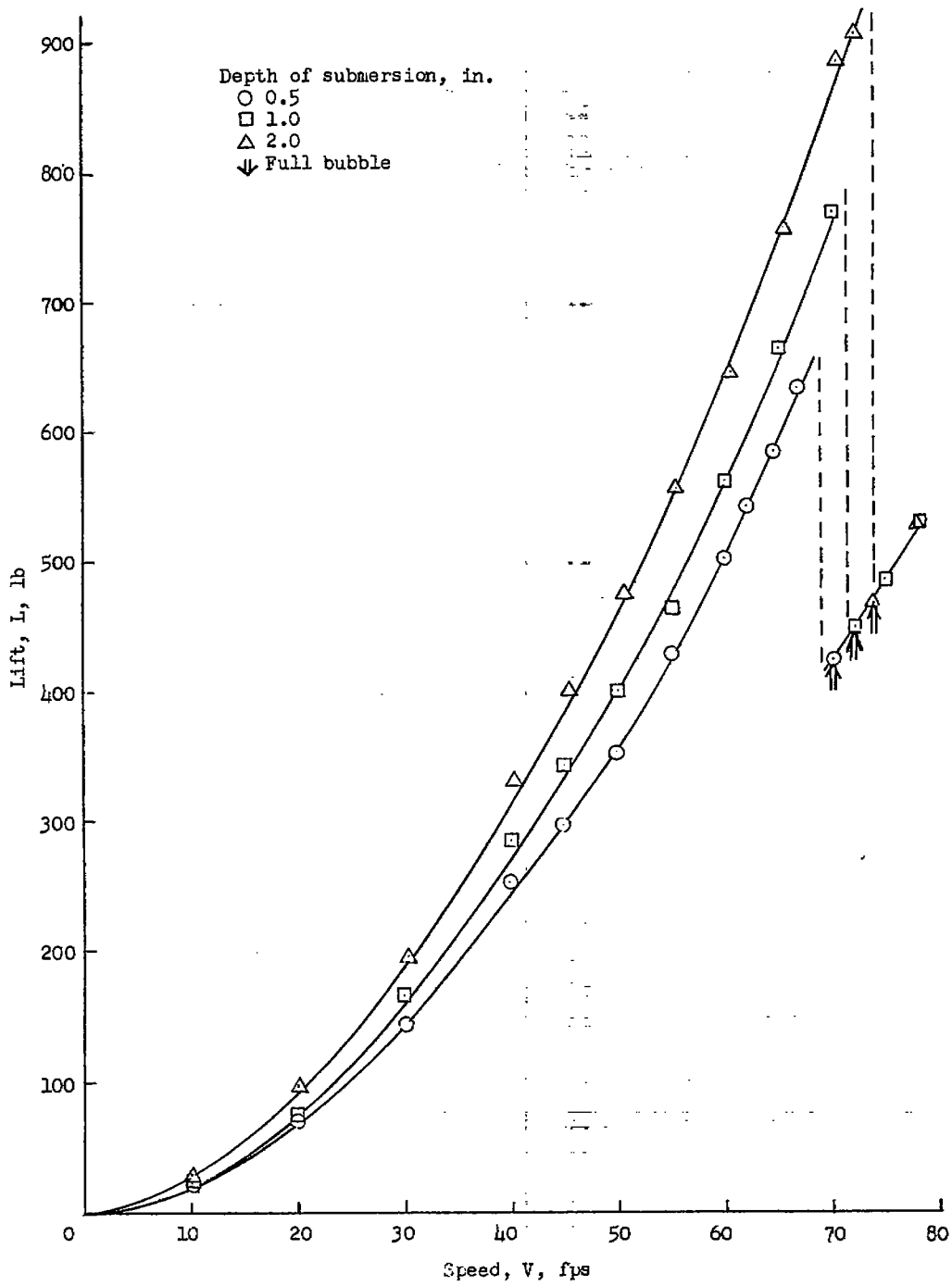
Figure 6.- Lift-force data for large model illustrating effects of low-
angle bubble. (Angle of attack, 8°.)
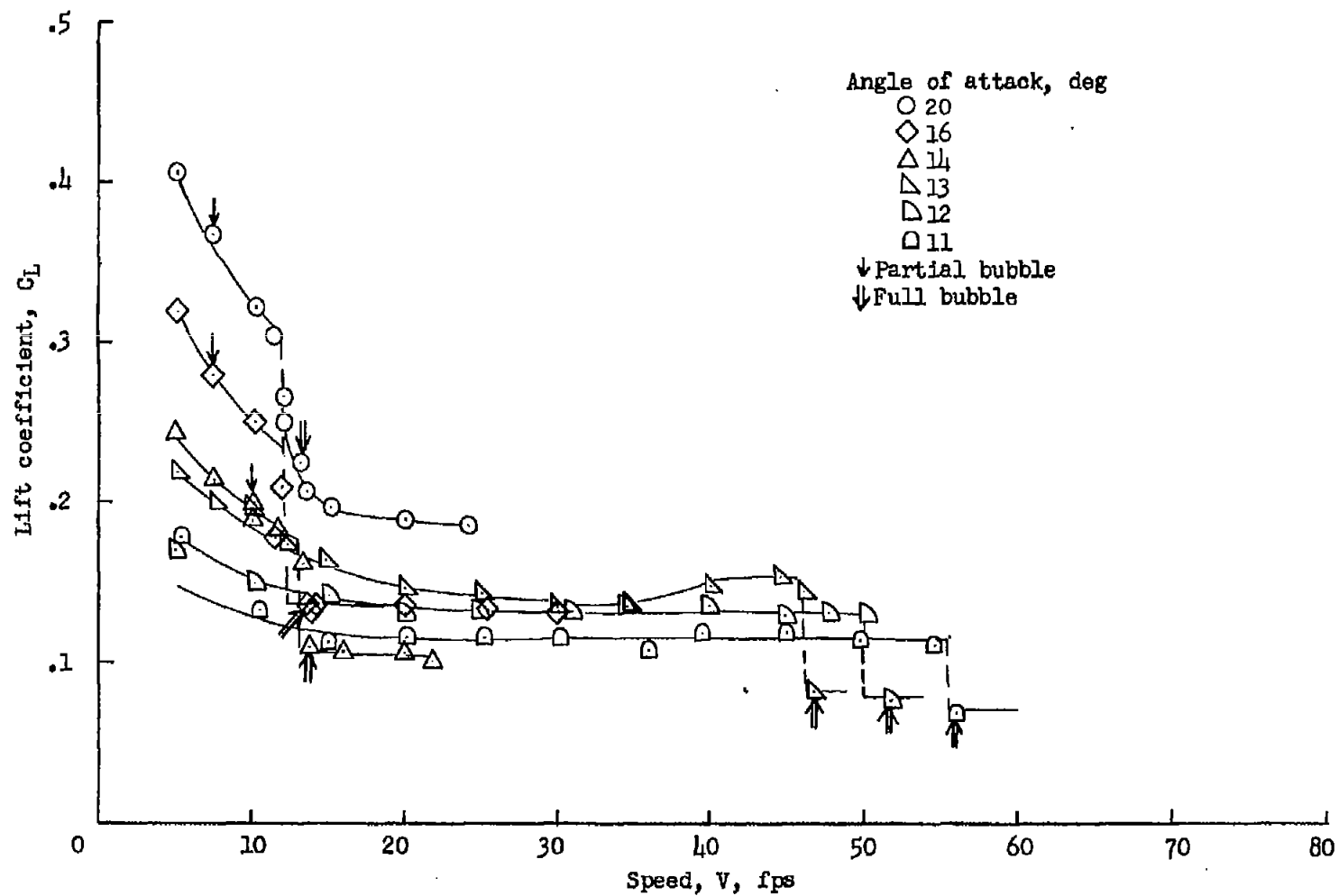
(a) Depth of submersion, 0.5 inch.

Figure 7.- Lift characteristics of small model.
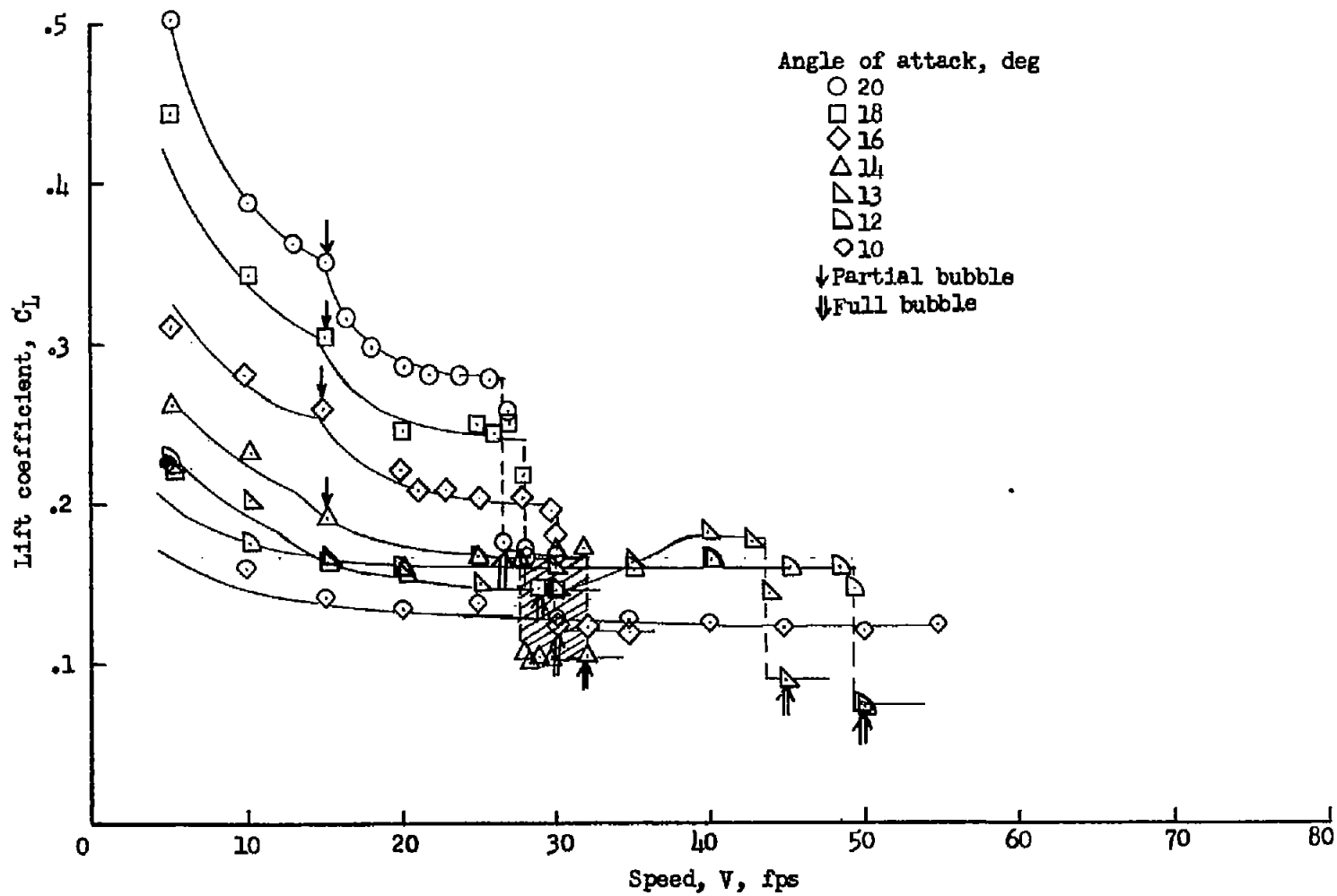
(b) Depth of submersion, 1.0 inch.

Figure 7.- Concluded.
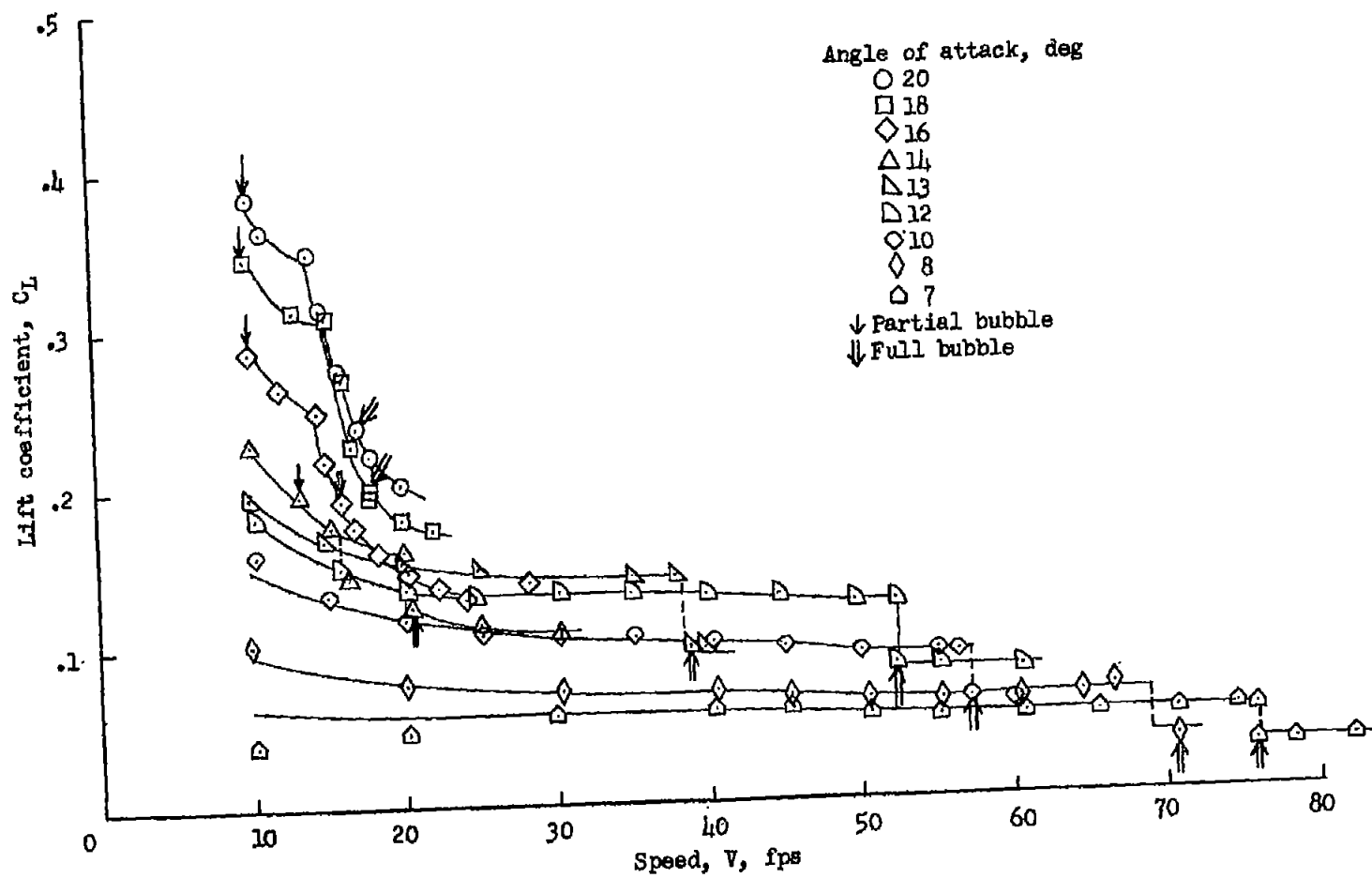
(a) Depth of submersion, 0.5 inch.

Figure 8.- Lift characteristics of large model.
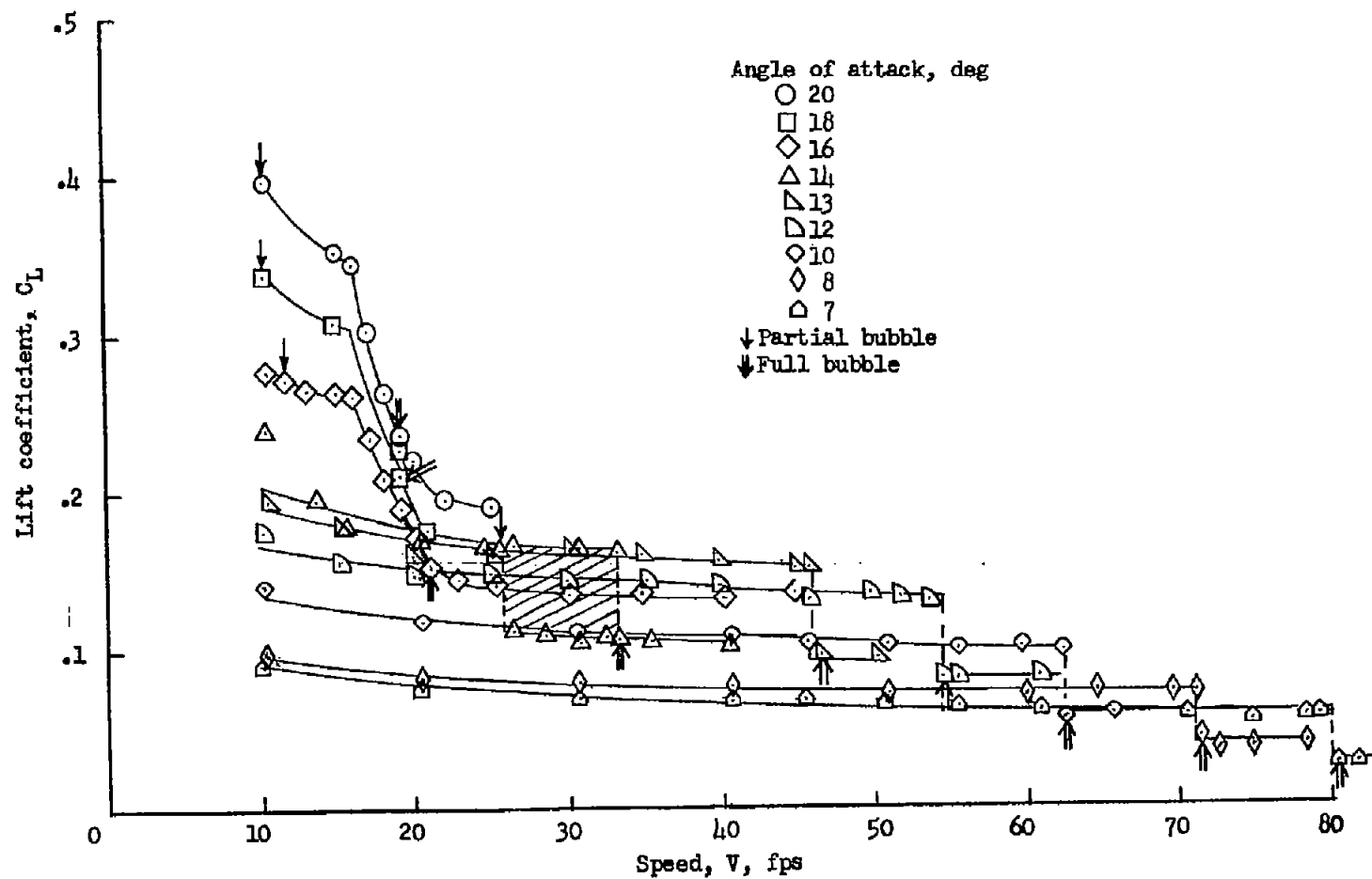
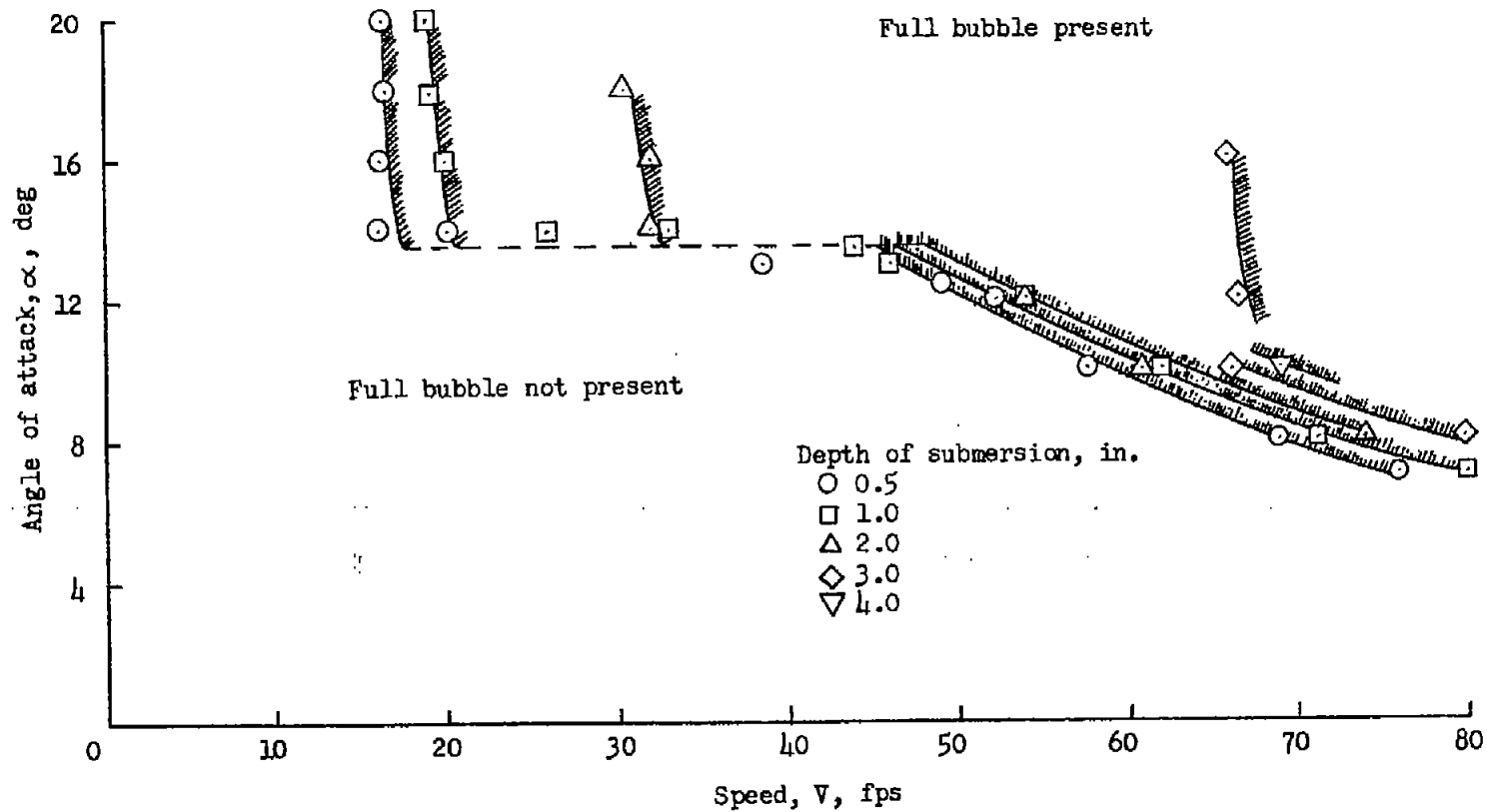(b) Depth of submersion, 1.0 inch.

Figure 8.- Continued.
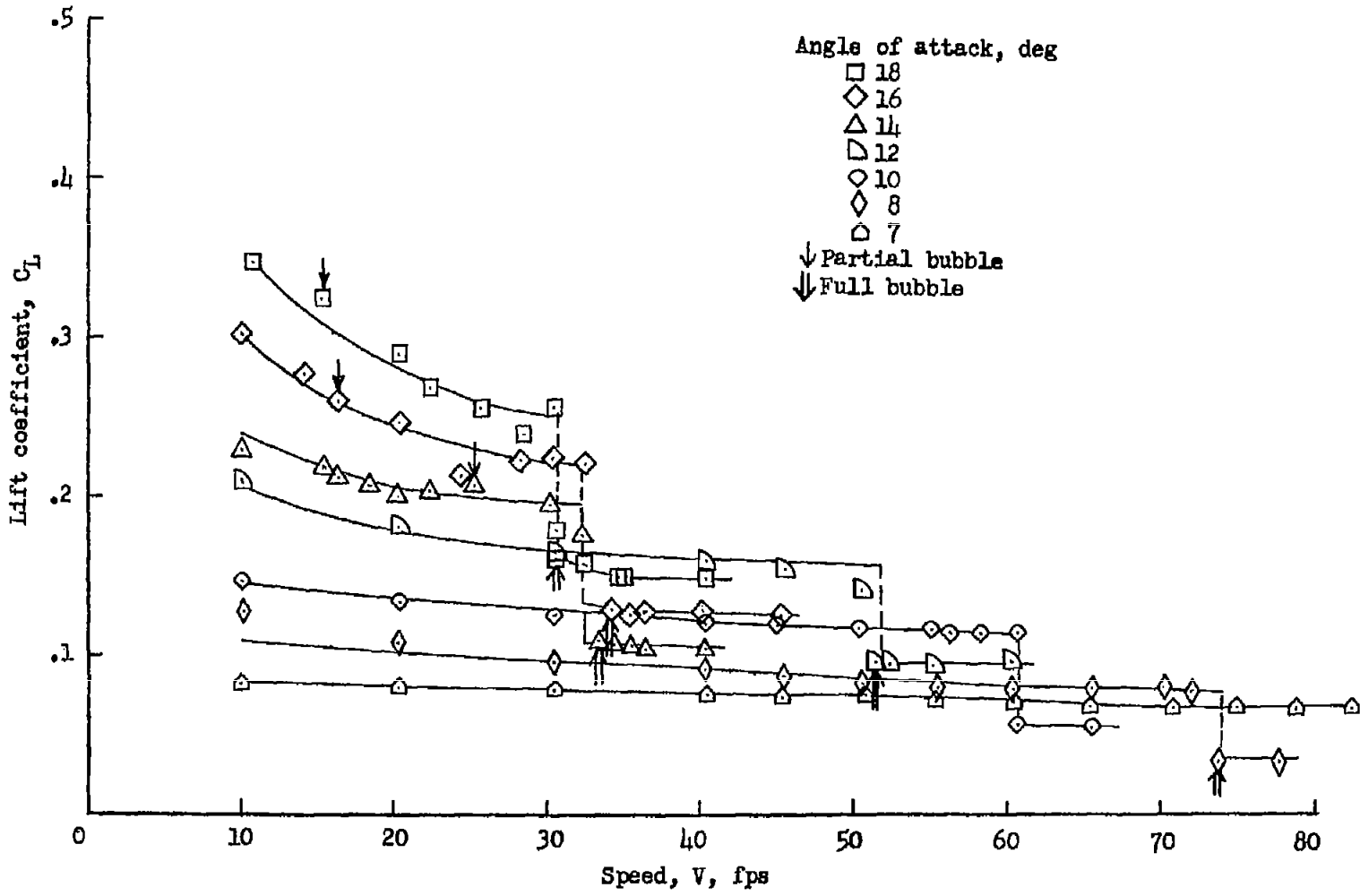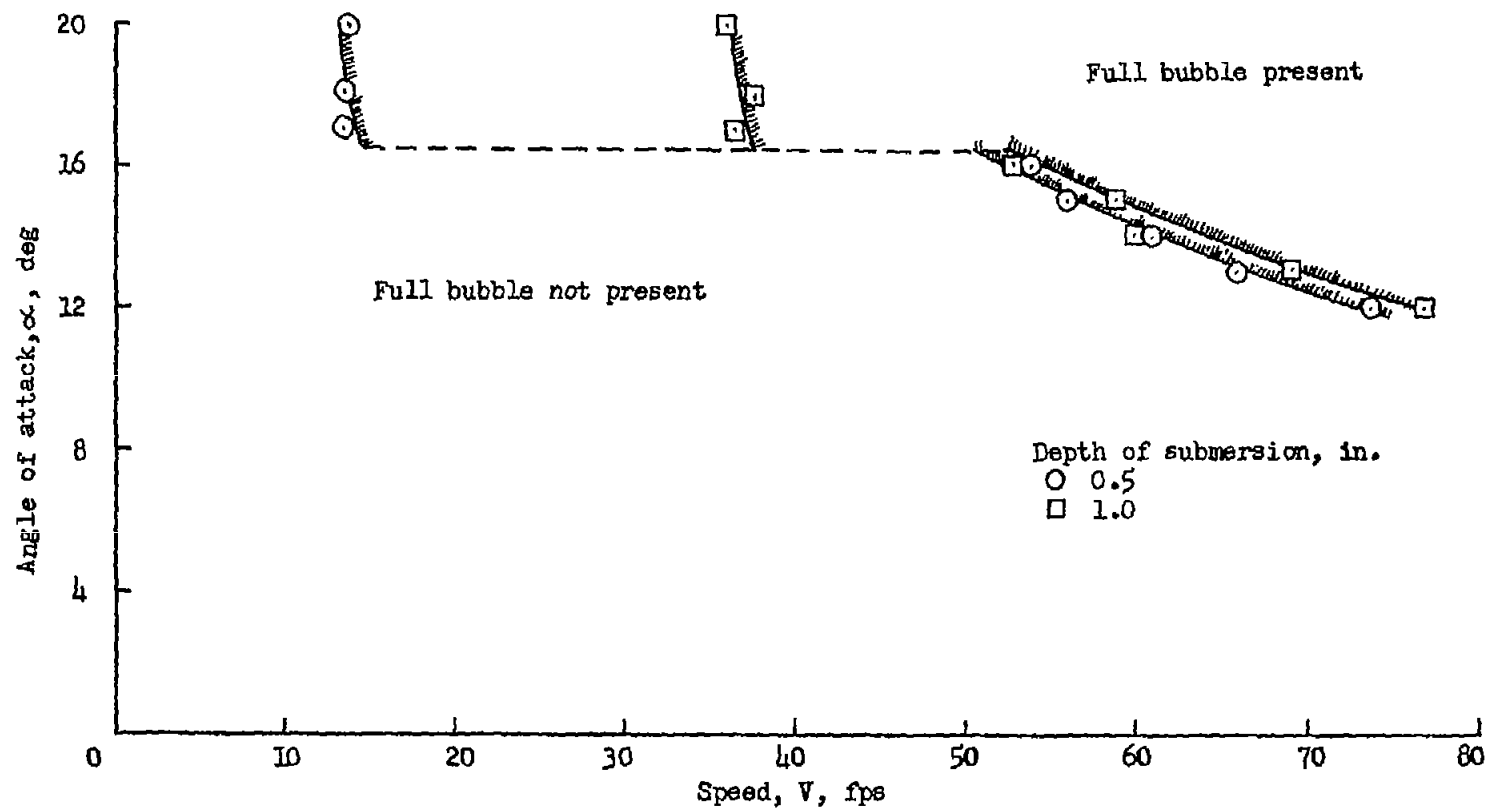
(c) Depth of submersion, 2.0 inches.

Figure 8.- Continued.
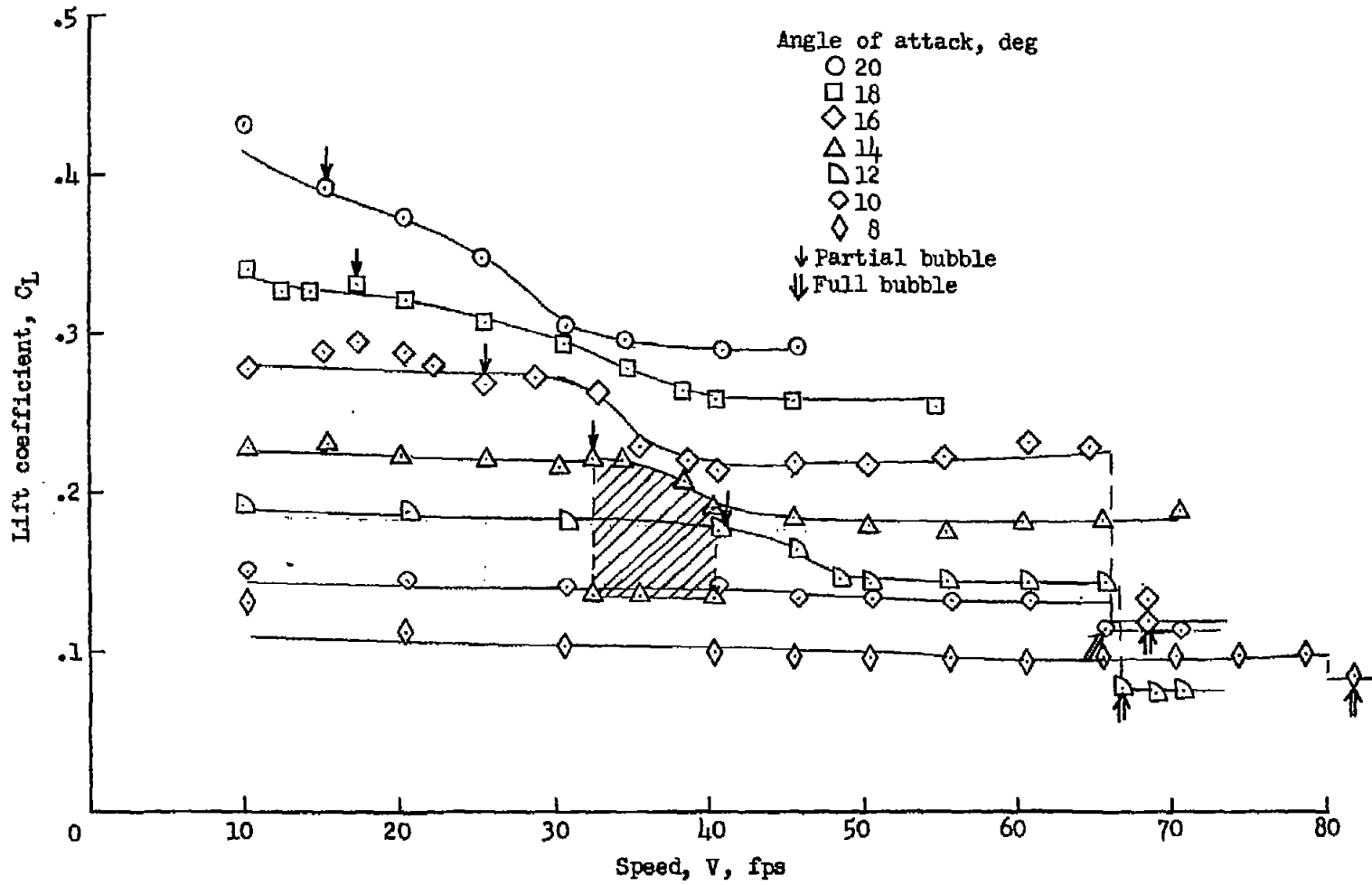
(d) Depth of submersion, 3.0 inches.

Figure 8.- Continued.
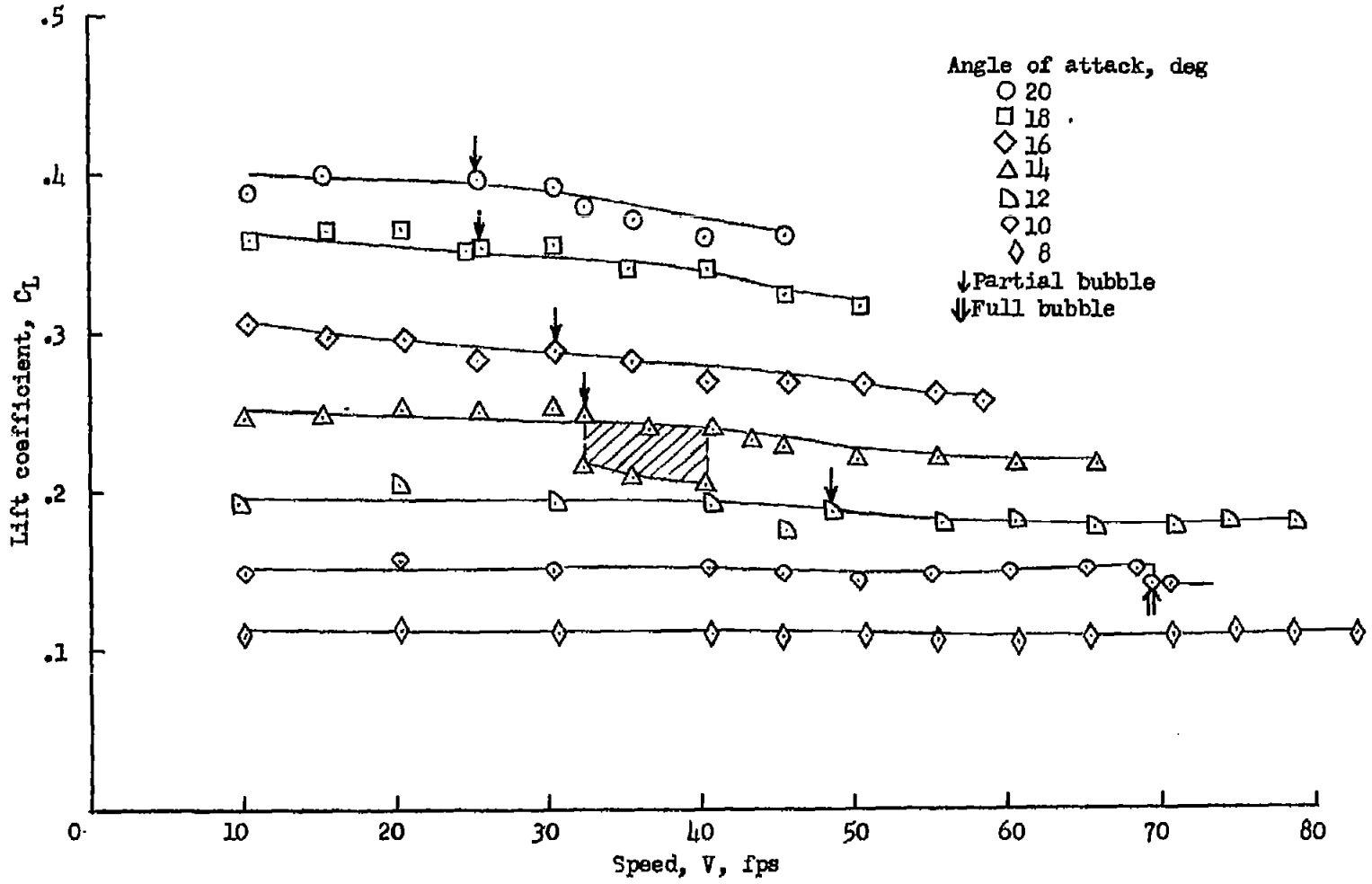
(e) Depth of submersion, 4.0 inches.

Figure 8.- Continued.
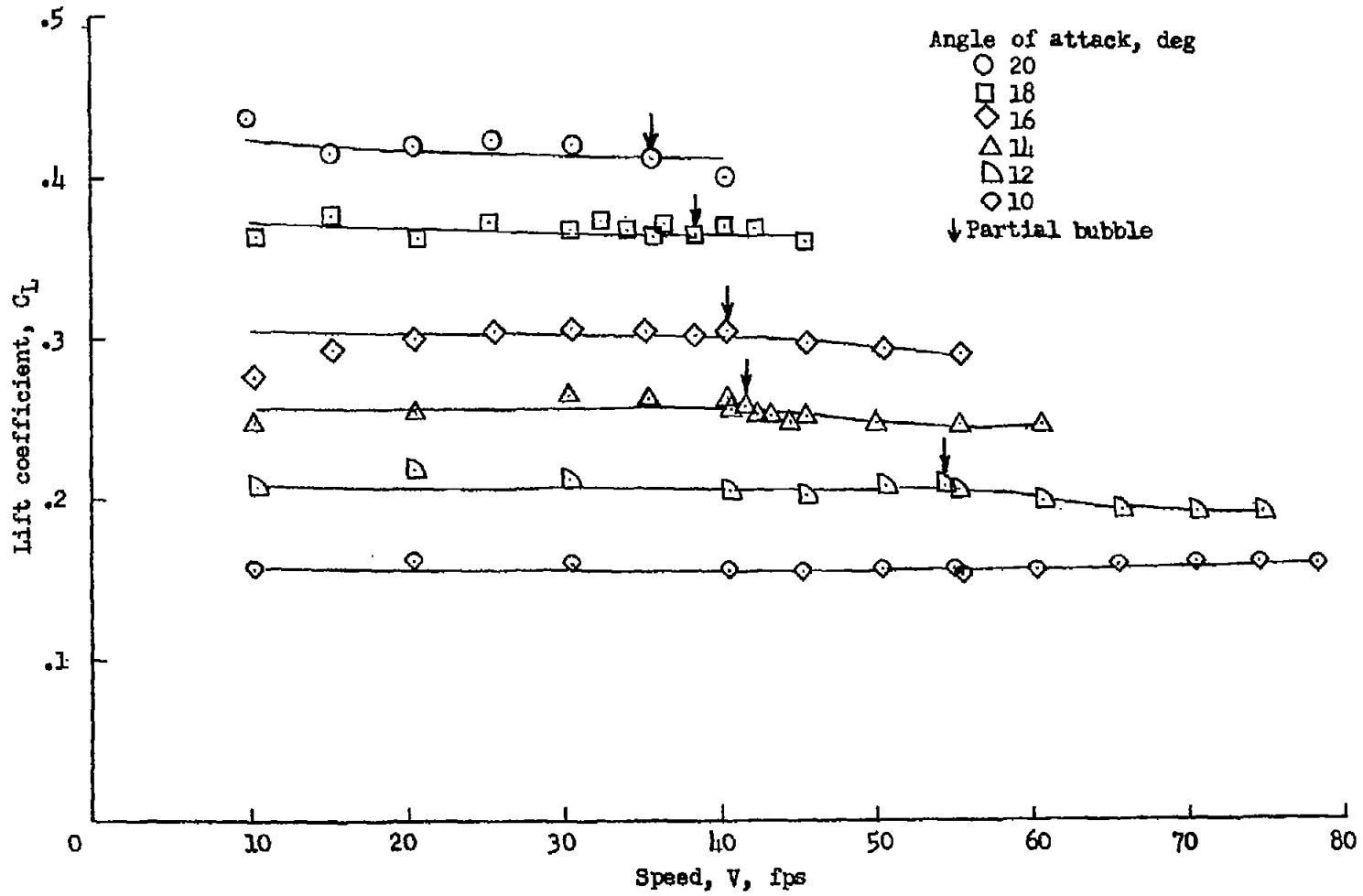
(f) Depth of submersion, 5.0 inches.

Figure 8.- Concluded.
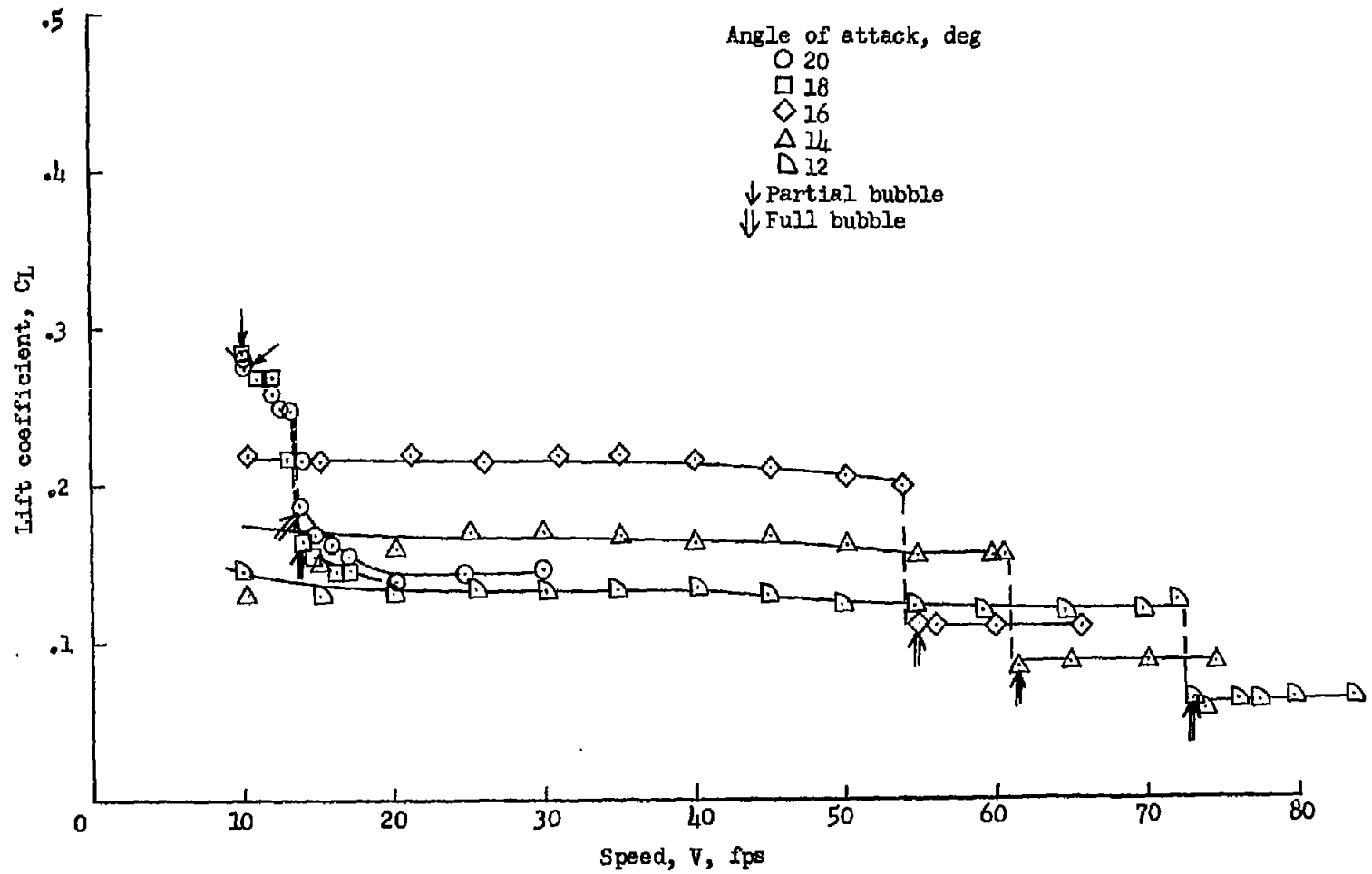
(a) Depth of submersion, 0.5 inch.

Figure 9.- Lift characteristics of the thick model.
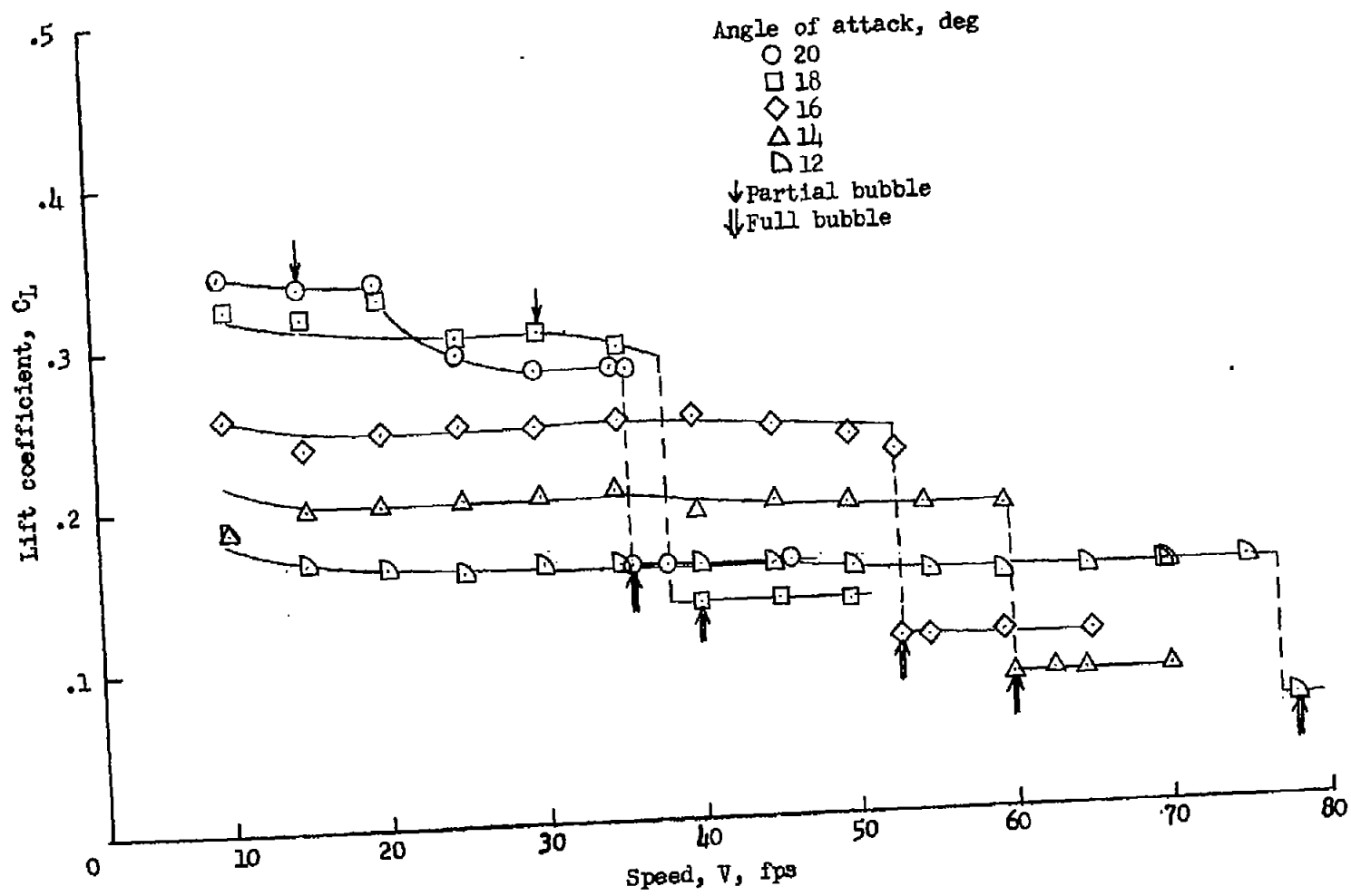
(b) Depth of submersion, 1.0 inch.

Figure 9.- Concluded.
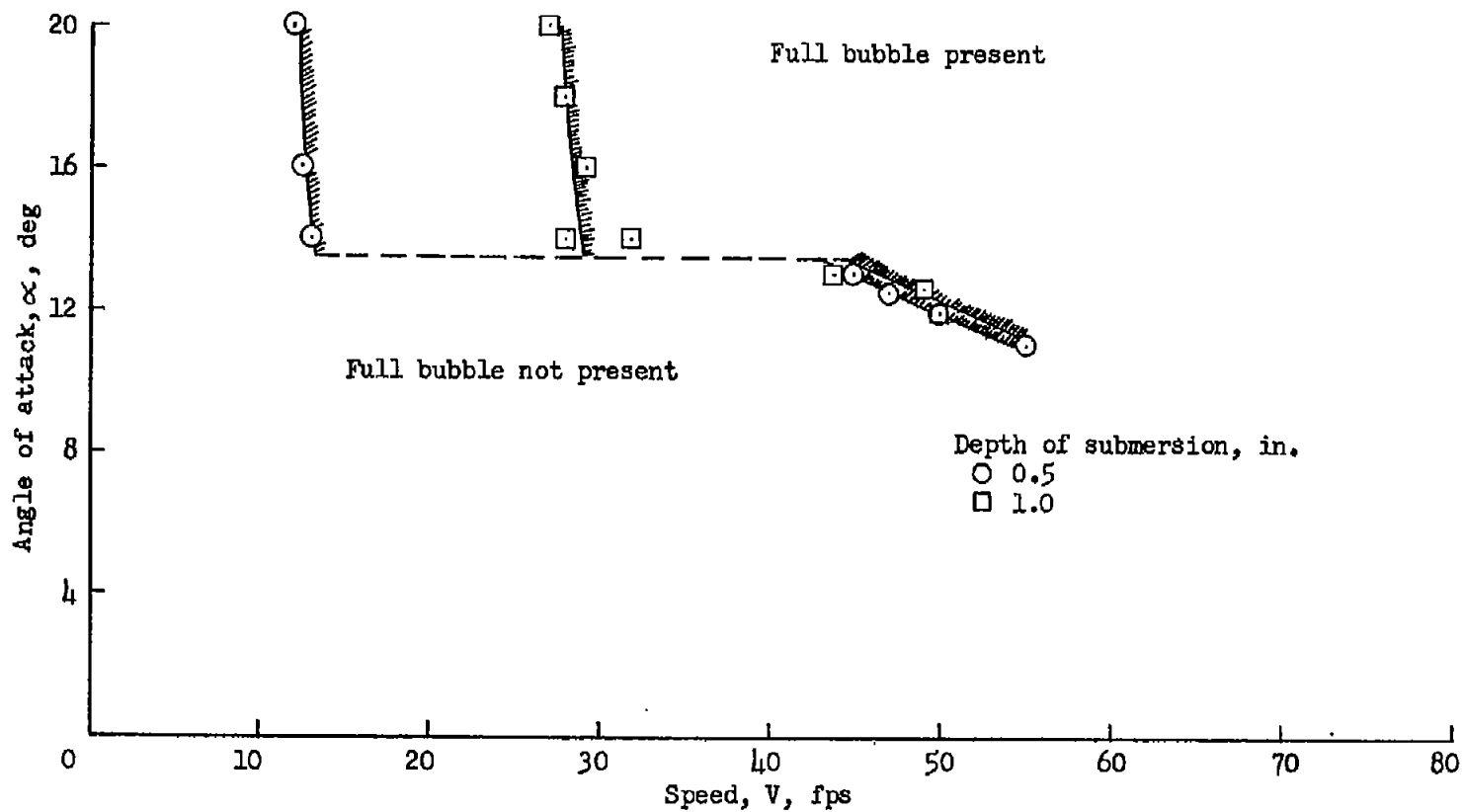
(a) Small model.

Figure 10.- The effect of depth of submersion on ventilation boundaries.

(b) Large model.

Figure 10.- Continued.

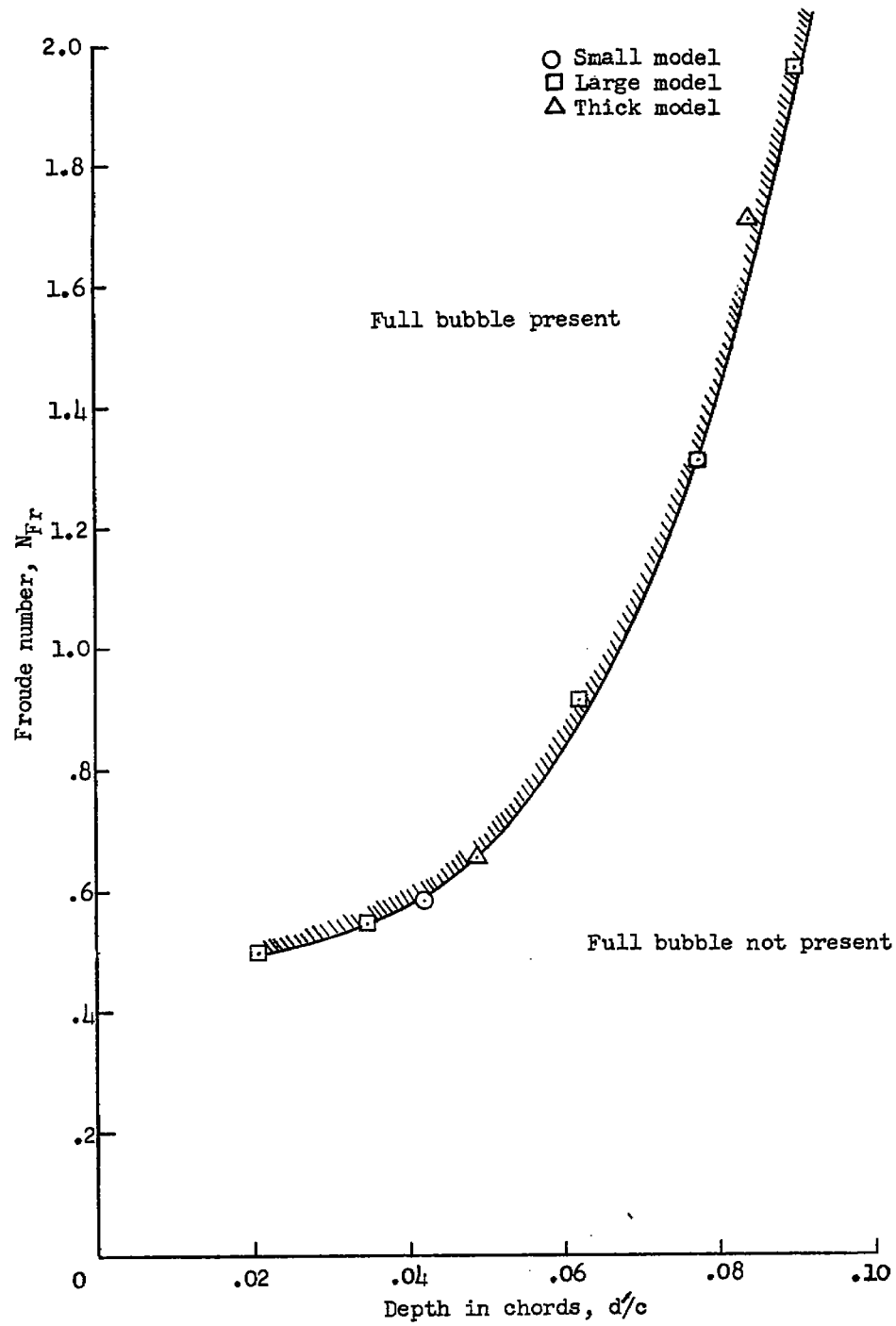(c) Thick model.
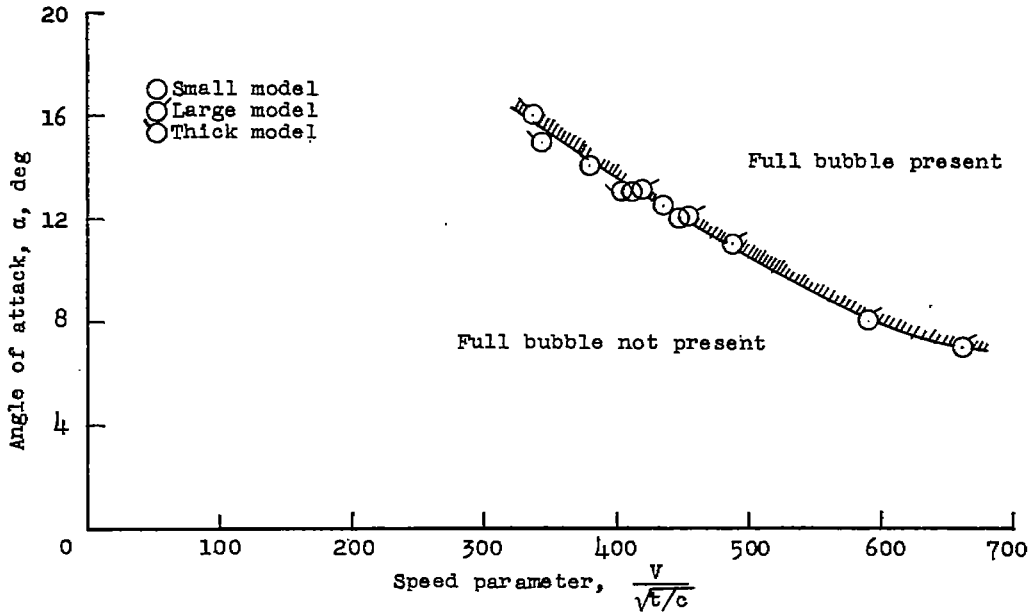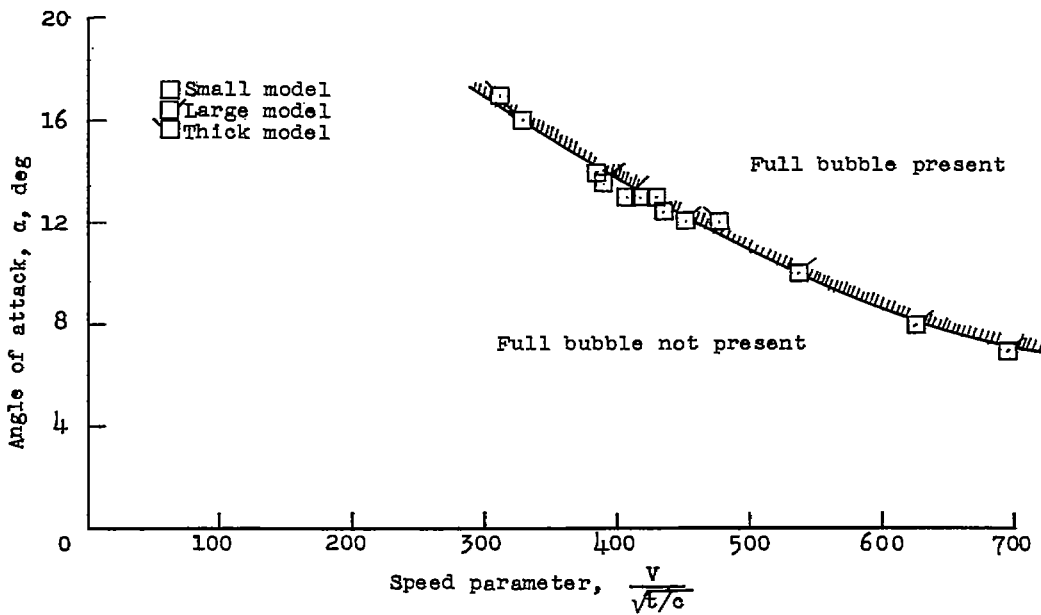
Figure 10.- Concluded.

Figure 11.- Correlation of ventilation speeds for the high-angle bubble.

(a) Depth of submersion d, 0.5 inch.

(b) Depth of submersion d, 1.0 inch.

Figure 12.- Correlation of ventilation speeds for the low-angle bubble.